A Novel Dual-Band Band-Pass Filter using Plasmonic Square Ring Resonator

P. Osman [1], P V Sridevi [2], K V S N Raju [3]

[1] *Department of Electronics and Communication Engineering*
Samuel George Institute of Engineering & Technology, Darimadugu, Markapur, Prakasam-Dt, Andhra Pradesh, India.
[2] *Department of Electronics and Communication Engineering*
A U College of Engineering (A), Andhra University, Visakhapatnam, Andhra Pradesh, India.
[3] *Department of Electronics and Communication Engineering*
S.R.K.R.Engineering College, Bhimavaram, Andhra Pradesh, India.

[1] pathanosman@gmail.com, [2] pvs6_5@yahoo.co.in, [3] Kvsn45@gmail.com

***Abstract* - We propose a plasmonic Metal-Insulator-Metal (MIM) waveguide based on a new ring resonator Band-Pass Filter (BPF) with tunable band-pass bandwidth. We use very easy techniques for analyzing the resonant frequencies and transmission coefficients. The band-pass filter operates at optical wavelengths in between O & L bands. To design band-pass filters, stepped-impedance stubs with open lengths are connected with the ring to acquire the tunable bandwidth. A full wave simulation software tool is used in the design of the band-pass filter. The filter has wide applications in high density Photonic Integrated Circuits (PICs).**

Keywords - Plasmonics, MIM Waveguides, Ring-Resonators, PICs.

I. INTRODUCTION

Surface plasm on polaritons (SPPs) are the basic elements for propagating the electromagnetic waves which have been generated and enclosed in the surface of the metal-dielectric interface [1], which are also known to be overcome the diffraction limit in the light at nano-scale domain [2]. Recently, nano-plasmonic metal-insulator-metal (MIM) waveguide is one of several research topics [3], [4], which can be confirmed to be a more effective technique for guiding the light with nanoscale mode confinement and comparatively low loss [5], [6]. Being well recognized, several subwave lengths optical devices have been designed using nano-plasmonic MIM waveguide are generally studied and reported [7]-[11], which can be obtained by simply coupling with different resonators. Various stub resonators are already studied and researched by theory and experiments, including tooth-shaped MIM waveguides [12-13], disk-resonators [14], triangular-ring resonators [15], rectangular ring [16], square ring [17], and circular ring [18]. Still, most of these stub resonators are the symmetrical shape. Keeping this fact in mind, we have newly proposed a nano-plasmonic ring resonator based band-pass filter at optical frequency bands.

This paper describes the ring resonator with step impedance resonator for the first time and investigates a nano-scale plasmonic band pass filter at optical wavelengths. The full-wave simulations are used to study the transmission performance of the proposed system using CST Microwave studio suite. The step impedance resonator with open lengths used to analyze the dual-band nature at optical wavelengths. Moreover, the transmission spectrum of all dual-band band-pass filter is realized in the circular ring resonator with two fed-lines when the refractive index of the insulator and the inner radius of the ring resonator are fixed. Additionally, thie wavelengths and transmission spectrum of the dips and peaks are discussed. The transmission and reflection coefficients of the nano-plasmonic MIM waveguide-based optical devices have been obtained at THz frequencies with a controllable transmission spectrum, which contains potential application in photonic integrated circuits (PICs) [19].

II. BAND PASS FILTER BASED ON STEP IMPEDANCE RING RESONATOR

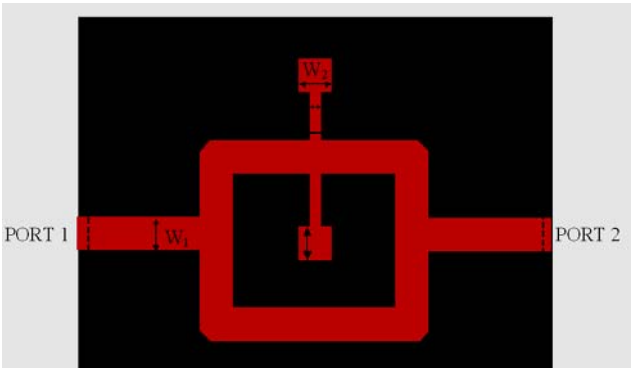

Fig. 1. Geometry of Band Pass Filter (BPF) using Square Ring Resonator of fixed lengths: L_1 =1800mm, L_2 = 720mm, L_3 = 345mm and fixed Widths: W_1 = 210mm, W_2 = 82mm, W_3 = 152mm.

The proposed device have been designed by using CST Microwave studio suite. The step impedance ring resonator

based band pass filter is analyzed and the results shown that they have dual bands in the transmission spectrum of optical frequencies. Moreover, the transmission spectrum of BPFs is realized in the SRR design with step impedance resonator when the refractive index of the insulator and the inner radius of the ring resonator are fixed. We carry out the full-wave simulation with dimensions, a perfect matched layer (PML) boundary conditions, time step ($\Delta t = \Delta x/2c$, c is the velocity of light in vacuum), mesh sizes are 5-nm × 5-nm. To simplify the calculation, the metal and insulator are assumed to be silver and silica, respectively. The parameters for the silver and silica can be fixed as $\varepsilon_\infty = 3.7$, $\omega_p = 1.38 \times 10^{16}$ rad/s, $\Upsilon = 2.73 \times 10^{13}$ rad/s and $\varepsilon_i = 2.50$ (silica) that are obtained by fitting experimental results [20].

The design of an SRR have two similar step impedance type stubs fed by directly parallel coupled lines have shown in Fig. 1. Both of these open lengths, step impedance stubs contain narrow and wide parts, which can be positioned on the equal plane to disturb the ring resonator. Fig. 1 contains the characteristic impedance $Z_1$of two fed-lines along with the square ring resonator, whereas Z_2 and Z_3 those of the step impedance stub. The electrical length of one-quarter of the ring denoted by θ_1, while $\theta_2$and $\theta_3$are electrical lengths of the both sections of the open stubs respectively. By adding two similar open length stubs, it can easily achieve large tunable states of the band-pass band-width.

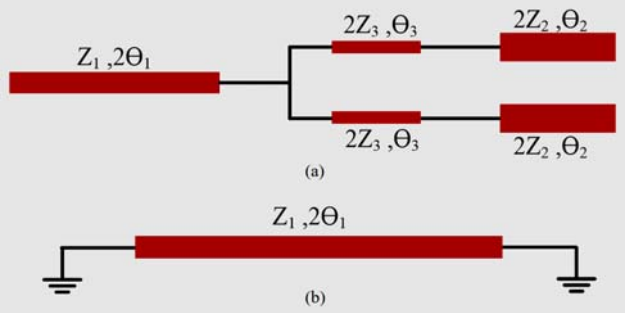

Fig. 2. Equivalent circuit of BPF using Square Ring Resonator of: (a) Even Mode, (b) Odd Mode.

The even- and odd-mode circuits have been used to determine the BPF resonant frequencies [6]. By using the symmetric plane like open and short circuit for even and odd modes, the geometry of the Fig. 1 has been divided. Fig. 2 (a) shows the result from step impedance stubs in half along the plane of the symmetry. Fig. 2 (b) shows the equivalent circuit which is drawn for the plane of the symmetry as a ground plane. The resonant frequencies have been investigated from one end of the even- and odd-mode circuit respectively, when $Yin = 0$ and $Zin = 0$, which can be given by:

For even modes:

$$K + k\cot\theta_2 \tan\theta_2 + K\tan 2\theta_1\left(k\cot\theta_2 - k\tan\theta_3\right) = 0 \quad (1)$$

For odd modes:

$$\tan 2\theta_1 = 0 \quad (2)$$

where K and k are impedance ratios Z_2/Z_1 and Z_3/Z_1 respectively

The transmission peaks can be calculated when $Y_{21} = Y_{12} = 0$, by adding higher and lower admittances of the two paths connected in between two fed-lines shown in Fig.1. The transmission zeros are obtained and calculated results have been shown in Fig. 1 and it can be expressed by:

$$\left\{\cos\theta_1 - \frac{\sin\theta_1}{K}\frac{K + k\cot\theta_2 \tan\theta_3}{k\cot\theta_2 - K\tan\theta_3}\right\}^{-1} + \sec\theta_1 = 0 \quad (3)$$

The electrical length $\Theta_1$can decides easily by using both the center frequencies and substrates transmission [12], [13] shown in Fig. 1. The length and widths of the stubs are chosen to be l_1 = 1800-nm w_1 = 210-nm for the center frequency 205-THz. A 50-ohm waveguide has been used for Z_1. The rest of the 4-variables such as θ_2, θ_3, Z_2, and Z_3, are not only used for BPF characteristics and it will be useful for calculating tunable and band-pass characteristics. These undetermined values can be predicted by using the earlier three conditions (1)-(3).

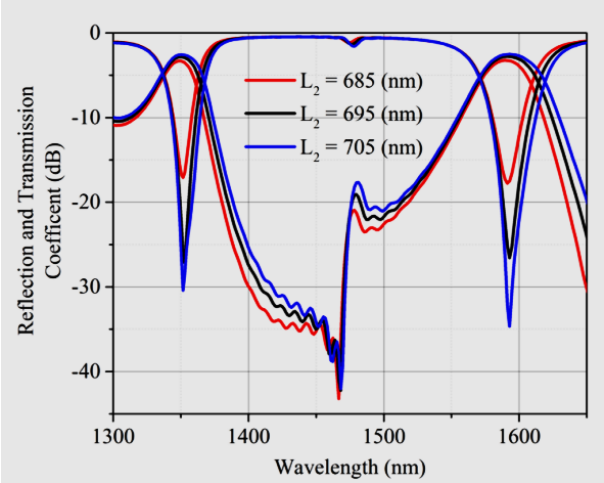

Fig.3. Variation in Reflection and Transmission Coefficient of BPF using Square Ring Resonator of Length L_2 as a function of wavelength.

Simulated SRR results are fed by the direct connection feed-lines shown in Fig. 3. To obtain the results of the SRR through direct fed-lines have been found by using dimensions of ring resonator θ_2/θ_1=, $\theta_2/\theta_1 = \theta$, that is l_1= 1800-nm, l_2 = 720-nm, l_3 = 345-nm. Also, the physical widths of the lines are selected as follows; w_1 = 210-nm ,w_2 = 82-nm,w_3 = 152-nm . The transmission coefficients of the inter digital lines are towards transmission peaks of the SRR

at about 188 and 222 THz. The result of these types of overlaps is usually exhibited if the ring and the inter-digital coupled lines have been used with each other. The simulations have done by using the same physical dimensions of the ring and the two-step impedance stubs shown in Fig. 3. The over laps of zeros and peaks have been shown in Fig. 6 with improved sharp rejections and stop bands at cut off regimes. The magnitudes of electric fields have been shown in Fig. 4.

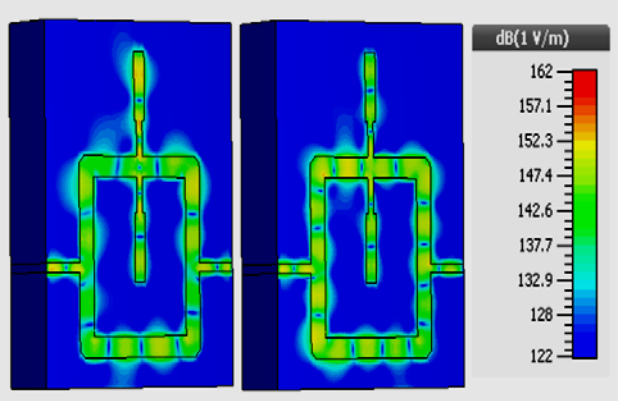

Fig. 4. Field Pattern of BPF using Square Ring Resonator at Wavelength : (a) 1581nm, (b) 1351nm.

III. DISCUSSION AND CONCLUSION

An ideal dual-band plasmonic Metal-Insulator-Metal (MIM) waveguide based Band-Pass Filter (BPF) with tunable pass-bands was designed by using multiple step impedance open length stubs and inter digital fed-lines. Each section of the BPF was designed by step impedance stubs connected to the Square Ring Resonator (SRR) which was created by determining the resonant and transmission zero frequencies attained from the equivalent circuits. Wide- and narrow-band BPFs were designed by adjusting the range of resonances within the pass-bands with simultaneous increases or decreases of each width of the step impedance open length stubs. The transmission peaks were explained by the resonance condition, which agrees well with the numerical simulation and theoretical calculation. Our research reported in this paper provides a promising application of plasmonic dual band-BPFs and plasmonic integrated optical circuits.

REFERENCES

[1] W. Mu and J. B. Ketterson, "Long-range surface plasmon polaritons propagating on a dielectric waveguide support," Opt. Lett., vol. 36, no. 23, pp. 4713-4715, Dec. 2011.

[2] W. Liu, R. Zhong, J. Zhou, Y. Zhang, and M. Hu, "Investigations on a nano-scale periodical waveguide structure taking surface plasmon polaritons into consideration," J. Phys. D: Appl. Phys. vol. 45, no. 20, pp. 205104 (1-9), May 2012.

[3] P. Taylor, C. Li, D. Qi, J. Xin, and F. Hao, "Metal-insulator-metal plasmonic waveguide for low- distortion slow light at telecom frequencies," J. Modern Opt. Vol. 61, no. 8, pp. 37-41, Nov.2014.

[4] R. Zafar and M. Salim, "Analysis of asymmetry of Fano resonance in plasmonic metal-insulator-metal waveguide," J.photonics, vol. 23, pp. 1-6, Nov. 2016.

[5] J. H. Zhu, Q. J. Wang, P. Shum, and X. G. Huang, "A Simple NanometericPlasmonic Narrow-Band Filter Structure Based on Metal-Insulator-Metal Waveguide," IEEE Trans. on Nanotech., vol. 10, no. 6, pp. 1371-1376, Nov. 2011.

[6] B. H. Cheng, Y. Lai, and Y. Lan, "Plasmonic Photonic Bloch Oscillations in Composite Metal -Insulator -Metal Waveguide Structure," Plasmonics, vol. 9, no. 1, pp. 137-142, Jul. 2013.

[7] G. Veronis, S. Fan, and S. Member, "Modes of Subwavelength Plasmonic Slot Waveguides," J. Lightwave Tech., vol. 25, no. 9, pp. 2511-2521, Sept. 2007.

[8] A. Hosseini, A. Nieuwoudt, and Y. Massoud, "Efficient simulation of subwavelength plasmonic waveguides using implicitly restarted Arnoldi," Opt. Express, vol. 14, no. 16, pp. 487-494, Aug. 2006.

[9] M. Wu, Z. Han, and V. Van, "Conductor-gap-silicon plasmonic waveguides and passive components at subwavelength scale," Opt. Express, vol. 18, no. 11, pp. 11728-11736, May 2010.

[10] D. F. P. Pile and D. K. Gramotnev, "Plasmonic subwavelength waveguides : next to zero losses at sharp bends," Opt. Lett., vol. 30, no. 10, pp. 1186-1188, May 2005.

[11] N. Podoliak, P. Horak, J. C. Prangsma, and P. W. H. Pinkse, "Subwavelength Line Imaging Using Plasmonic Waveguides," IEEE J. Q. Elct., pp. 7200107-7200107 , vol. 51, no. 2, Feb. 2015.

[12] X. Lin and X. Huang, "Numerical modeling of a teeth-shaped nanoplasmonic waveguide filter," J. Opt. Soc. Am. B, Vol. 26, pp. 1263-1268, 2009.

[13] H. Lu, X. Gan, D. Mao, and J. Zhao, "Graphene-supported manipulation of surface plasmon polaritons in metallic nanowaveguides," Photon. Res. Vol. 5, pp. 162-167 , 2017.

[14] H. Lu, X. Liu, D. Mao, L. Wang, and Y. Gong, "Tunable band-pass plasmonic waveguide filters with nanodisk resonators," Opt. Express Vol. 18, pp. 17922-17927, Aug. 2010.

[15] G. Oh, D. Kim, S. H. Kim, H. C. Ki, T. U. Kim, and Y. Choi, "Integrated Refractometric Sensor Utilizing a Triangular Ring Resonator Combined With SPR," IEEE Pho. Tech. Lett., vol. 26, no. 21, pp. 2189-2192, Nov. 2014.

[16] B. Yun, G. Hu, and Y. Cui, "Theoretical analysis of a nanoscale plasmonic filter based on a rectangular metal – insulator – metal waveguide," J. Phy., vol.43, no. 38, pp. 385102 (1-8), Nov. 2010.

[17] J. Liu, G. Fang, H. Zhao, and Y. Zhang, "Plasmon flow control at gap waveguide junctions using square ring resonators," J. Phy., vol.43, no. 5, pp. 055103 (1-6), Nov. 2009.

[18] A. Setayesh, S. R. Mirnaziry, and M. S. Abrishamian, "Numerical Investigation of Tunable Band-pass \ band-stop Plasmonic Filters with Hollow-core Circular Ring Resonator," J.Opt. Soc. of Korea, vol. 15, no. 1, pp. 82-89, Mar. 2011.

[19] K. Murali Krishna, Md. Zia Ur Rahman, Shaik Yasmin Fathima, "A New Plasmonic Broadband Branch Line Coupler for nanoscale Wireless Links", IEEE Photonic Technology Letters, vol. 29, no. 18, pp. 1568-1571, 2017.

[20] M. Li, W. H. P. Pernice, C. Xiong, M. Hochberg, and H. X. Tang, "Harnessing optical forces in integrated photonic circuits," Nat. Lett., vol. 456, pp. 480-484, Nov. 2008.

[21] MortezaEbadiet. Al, High-Efficiency Nanoplasmonic Wavelength Filters Based on MIM Waveguides. IEEE Potn. Tech. Lett., Vol. 28, pp. 2605-2608, 2016.

[22] Jhonson and Christy, "Optical Constants of Noble Metals, " Phys. Rev. Lett., vol.6, no. 12, pp. 4370-4379, Dec. 1972.

[23] C. H. Kim and K. Chang, "Ultra-Wideband (UWB) Ring Resonator Bandpass Filter With a Notched Band," IEEE Micro. Wirel. Comp. Lett., vol. 21, no. 4, pp. 206-208, Apr. 2011.

.